Vol. 42, No. 4 (2020) 627-640, DOI: 10.24874/ti.966.09.20.11

Tribology in Industry

www.tribology.rs

RESEARCH

Control of the Exhaust Gas Tract Resistance of Modern Engines by the Run-Down Time during Testing

A. Gritsenko[a,b], V. Shepelev[a,*], K. Lukomsky[c], F. Grakov[b], N. Kostyuchenkov[d], O. Kostyuchenkova[d]

[a]*Department of Automobile Transport, South Ural State University, Chelyabinsk, Russia*
[b]*Department of Machine-Tractor Fleet Operation, South Ural State Agrarian University, Troitsk, Russia*
[c]*Air Force Academy named after professor N.E. Zhukovsky and Yu. A. Gagarin, Chelyabinsk, Russia*
[d]*Department of Agrarian Technique and Technology, S.Seifullin Kazakh Agrotechnical University, Nur-Sultan, Republic of Kazakhstan*

Keywords:

Car
Engine
Diagnostics
Test mode
Run-down
Rotation frequency
Technical condition

* Corresponding author:

Vladimir Shepelev
E-mail: shepelevvd@susu.ru

Received: 18 September 2020
Revised: 28 October 2020
Accepted: 18 November 2020

A B S T R A C T

The toxicity standards of modern cars are constantly tightening. Such standards can be reached only when using special systems and assemblies. The existing diagnostic methods are too time-consuming and do not exclude possible multiple errors. The article proposes a method for diagnosing the ICE (internal combustion engine) exhaust system of cars by the run-down time in test modes. An active study of possible diagnostic parameters allowed us to identify a sensitive diagnostic parameter – the run-down time. As the resistance of the catalytic converter increases, the run-down time decreases significantly. The experimental test showed the following: 1) when the run-down starts from 5,000 rpm, the run-down time in case of reaching the limiting resistance of the catalyst is halved - from 4.8 to 2.4 s; 2) in case of a limiting change in the resistance of the catalytic converter from 34 to 10 mm in the exhaust gases, the O_2 content increases from 2.53 to 4.92 %, the CO_2 content decreases from 13.17 to 12.57 %, and there is a sharp decrease in CH from 100 to 8 ppm. The run-down parameters control range is from 15 to 0.1 s. The production test of the new method for diagnosing the ICE exhaust system showed its significant performance.

1. INTRODUCTION

The widespread introduction of toxicity standards has significantly influenced the design and functions of the exhaust system of modern cars worldwide [1-3]. All the necessary environmental standards can be met only if cars are equipped with multicomponent closed-cycle catalysts and the ICE control system [4-7]. Besides, monitoring of the exhaust system elements serves the same purpose [8-10]. Currently, the exhaust system elements are very sensitive to changes in the fuel quality and worsening of the combustion process. Often, the declared long service lives of multicomponent catalysts of about 150-300 thousand km in practice show the first failures when running 50-100

thousand km [11]. New design elements of the exhaust system, such as the catalyst, impose significant uncertainty on the process of determining the technical condition of the ICE systems [12-14]. New failures are registered in combination with the known ones, and the existing diagnostic methods are insufficiently informative to recognize these combinations. Besides, the existing methods are too time-consuming and do not exclude possible errors [15].

To reduce significantly the harmful influence of non-serviceable exhaust systems on the operation of the vehicle's ICE and the environment, a new diagnostic method is needed, which would exclude possible diagnostic errors and reduce labor intensity. Many scientists and research teams have been engaged in the development of the ICE diagnosing methods and tools.

Zadrąg and Kniaziewicz proposed a methodology for the classification of acquired diagnostic parameters using the Hellwig's information capacity indicator method, which is the basis for building a ranking of diagnostic parameters based on the zero unitarisation method [16]. This methodology allows for the formulation of general conclusions and thus the wider application of collected empirical material.

Chepurnyi and Leonenko carried out theoretical and experimental studies to determine the main defects and malfunctions of ICE by analysing the parameters of the vibroacoustic signal [17]. It was shown that development of highly sensitive vibration sensors and inexpensive USB oscillographs allowed to simplify vibroacoustic method and to expand possibilities for the processing of the diagnostic data.

Murphy et al. used non-invasive technique developed for monitoring combustion pressure cycle related faults [18]. By means of the data on the crankshaft angular velocity received from a high-resolution encoder, a trained neural network is used to reconstruct the combustion pressure cycle curves. These reconstructed combustion pressure curves are then passed into another trained neural network for fault detection analysis.

Dawson et al. [19] presented is a method for model based diagnostics of automotive three-way catalysts (TWC). The model relates measurable engine inputs (engine air mass and catalyst temperature) to a metric indicating oxygen storage capacity. TWC diagnostics is realized using an information synthesis technique.

Antory applied a data-driven monitoring technique to diagnose air leaks in an automotive diesel engine [20]. Detailed investigations have shown that measured signals taken from the experimental test-bed often contain redundant information and noise due to the nature of the process. In order to deliver a clear interpretation of these measured signals, they therefore need to undergo a "compression" and an "extraction" stage in the modelling process. The status of the engine's performance is then monitored using this diagnostic model.

Desbazeille et al. focused on monitoring large diesel engines by analyzing the crankshaft angular speed variations [21]. First, the angular speed variations are modeled at the crankshaft free end. This includes modeling both the crankshaft dynamical behavior and the excitation torques. Mechanical and combustion parameters of the model are optimized with the help of actual data. Then, an automated diagnosis based on an artificially intelligent system is proposed. Neural networks are used for pattern recognition of the angular speed waveforms in normal and faulty conditions. An experimental fuel leakage fault is successfully diagnosed, including detection and localization of the faulty cylinder, as well as the approximation of the fault severity.

Kimmich et al. used semiphysical models of dynamic processes. They generated identification through the use of special neural networks of the signal model and the remainder of the parity equations [22]. Signal models and parity equations residuals are generated through the use of semiphysical dynamic process models and identification with special neural networks. Detectable deflections of these residuals lead to symptoms which are the basis for the detection of several faults.

Montes and Pisu used a fault detection method for the idle speed control of an internal combustion engine. [23] The proposed approach is based on residual generators using the parity equation and an active threshold calculation technique. Simulation results show 100 % fault detection during nominal temperature conditions, and 89.6 % fault detection during the initial operating stage of the engine.

Gennish et al. presented a new monitoring approach to diesel engine combustion based on acoustic measurement of exhaust systems [24]. It investigates the acoustic characteristics from the measurements of individual sensors and their combination based on a linear one port acoustic source model. The pressure waveform produces more accurate monitoring results for abnormal combustions such as those caused by faults in engine fuel injection systems.

You et al. carried out fault detection experiment by the PSO-BP NN (Particle Swarm Optimized Back Propagation Neutral Network) model to validate the method [25]. Experiment results show that the PSO-BP NN has more fast convergence speed and higher diagnosis accuracy than BP NN, and it provides a new fault detection method for engine inlet and exhaust system.

Let us briefly review the diagnostic methods and tools used to control the technical condition of the exhaust system. The tools to diagnose the ICE exhaust system are represented by motor testers, diagnostic scanners, oscilloscopes, gas analysers, special devices and accessories.

Motor testers are complex universal diagnostic tools [10-12]. As a rule, they implement the generalized control functions with possible expanding the diagnosis. They allow one to provide collection and display of ICE operation parameters, which are not controlled by electronic engine control system electronics. The advantage is their universality. The disadvantages include high price, a large number of controlled parameters, high labour intensity, and complexity of selective diagnostics.

Diagnostic scanners allow one to scan numerous parameters of the electronic control unit of a car, visualize system parameters, up to system variables of the control program [21]. Their advantage is low price, low labour intensity, universality for several car models. However, the disadvantages are the impossibility to analyse selectively the output parameters of individual ICE elements and the impossibility to analyse signals at specific points.

Today, mobile oscilloscopes are very popular among specialists in the field of car system diagnostics [8,917,24,25]. The advantage of digital oscilloscopes is spot checkability of any electronic elements of vehicle systems and their low cost. However, the disadvantages include significant labour intensity, the impossibility to monitor the parameters of the electronic control unit, the complexity of information analysis.

Gas analysers are widespread tools to control the exhaust system and other systems [16,19,23]. The advantage is high sensitivity to any changes in the technical condition of the ICE systems. However, there are many disadvantages: the complexity of the selective assessment of individual elements and systems, high cost, significant labour intensity to warm up the device.

We can outline the following devices in the group of special devices and appliances: exhaust gas leakage detectors, thermocouples as a single set and thermal imagers, pressure sensors in the exhaust manifold, and some others [18,20,22,23]. The main advantage is the selectivity of control by the diagnostic tools and low cost. Their disadvantage is the complexity of analysing the diagnostic information, low sensitivity to any changes in the technical condition, limited capabilities for complex diagnostics.

An important integral test element on modern cars is certainly the broadband sensor (lambda probe) [12,19,26]. Its advantage is that the sensor continuously detects changes in the mixture composition over a wide range. After that, the ECU almost instantly corrects the mixture composition for the current technical condition of the ICE. However, it is very difficult to determine the reason for the change in the mixture. Today, some models are already fitted with individual lambda probes in each manifold, which expands the possibilities of selective control. However, it is very difficult to highlight a specific element causing the malfunction from the complex of systems and elements.

Based on the analysis of the tools and methods used to diagnose exhaust systems, we established the insufficient efficiency of diagnostic technologies and tools. To improve the efficiency of the diagnostic process, we propose to use a new diagnostic method based on the value of the ICE run-down time. However, when implementing the new method, the relationship between the design and diagnostic parameters is uncertain. To reveal the uncertainty, we put forward a scientific

hypothesis: It is possible to determine the technical condition of the exhaust system (in particular, the catalytic converter) by measuring the value of the ICE run-down time.

We should consider the varieties of dynamic methods for assessing the technical condition of the ICE, diagnostic modes, and diagnostic parameters used for assessing the technical condition of the ICE (Fig. 1).

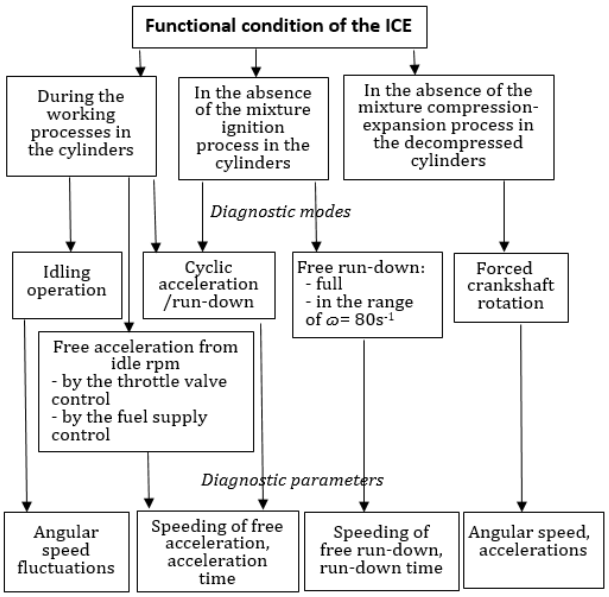

Fig. 1. Varieties of the dynamic methods for assessing the technical condition of the ICE, diagnostic modes, and diagnostic parameters used for assessing the technical condition of the ICE.

Figure 1 shows the varieties of dynamic methods used in modern technical di-agnostic means. As you can see, all the presented methods apply manipulations with the ICE crankshaft speed. The algorithms for their implementation have become widely used. However, no significant developments were found in the practice of diagnosing the exhaust system. To this end, we should consider the theoretical aspects of using the new method for diagnosing the exhaust system based on the ICE run-down time and check the ability to implement it in practice.

2. THEORETICAL RESEARCH

Before presenting a theoretical model linking the free run-down parameters, we should introduce some restrictions and consider the similarity of the run-down process of ICE turbochargers. A turbocharger has surely much smaller mass-overall dimensions and makes much more revolutions per minute. When the turbocharger (ICE crankshaft) rotates at a constant speed, the equation of the rotor (crankshaft) motion can be written as follows in the general form [27,28]:

$$J \cdot \frac{d\omega}{dt} = M_T - M_K - M_M \quad (1)$$

where $J \cdot \frac{d\omega}{dt}$ is the moment caused by the forces of inertia of the moving masses of the turbocharger rotor (crankshaft) (N·m); J is the moment of inertia of the rotor (crankshaft) relative to the axis (kg·m²); $\frac{d\omega}{dt}$ is the angular acceleration or deceleration of the rotor (crankshaft), depending on the operating mode (rad/s²); M_T is the effective torque developed by the turbine (ICE) (N·m); M_K is the moment consumed by the compressor (N·m); M_M is the moment of mechanical resistances to the rotor (crankshaft) rotation (N·m).

Using expression (1), we can express the deceleration of the rotor (crankshaft) in the form of:

$$\frac{d\omega}{dt} = \frac{M_T - M_K - M_M}{J} \quad (2)$$

When the turbocharger rotor (crankshaft) runs down, M_K and M_T are equal to zero, the equation of the rotor (crankshaft) motion in the run-down mode is as follows:

$$J \cdot \frac{d\omega}{dt} = -M_M \quad (3)$$

That is, the kinetic energy of the moving masses of the rotor (crankshaft) is spent to overcome the braking torque.

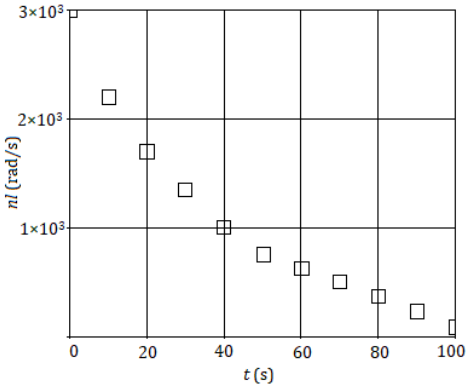

Fig. 2. The dependence of the rotation frequency *nl* on the time *t* at a free run-down of the turbocharger (crankshaft) rotor.

The experimental research carried out by Nosyrev et al [28] resulted in the graphic data used to build the dependence in Fig. 2. Let us take it as a theoretical one to study the relationship between the run-down time of the turbocharger rotor (crankshaft) and the rotation frequency.

The data in Fig. 2 was approximated by a quadratic equation with the approximation confidence of 0.95:

$$\omega(t) = 2817 - 55.8 \cdot t + 0.289 \cdot t^2 \quad (4)$$

where t is the run-down time (s).
Then, by calculating the first derivative of the speed, we obtained the deceleration:

$$\varepsilon = \frac{d\omega}{dt} = \omega(t) = -55.8 + 0.596 \cdot t \quad (5)$$

By multiplying equation (5) by the moment of inertia of the turbocharger (crankshaft) rotor, we obtained the braking torque (M).

$$M = J \cdot (-55.8 + 0.596 \cdot t) \quad (6)$$

The graphical interpretation of the dependences of the deceleration of the turbocharger (crankshaft) rotor $\varepsilon(t)$ and the braking torque M on the run-down time t is presented in Figs. 3a and 3b.

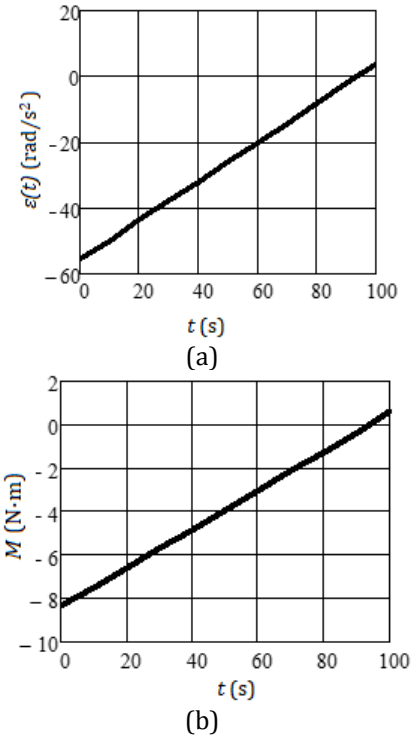

Fig. 3. The dependencies (a) of the deceleration of the turbocharger (crankshaft) rotor $\varepsilon(t)$ on the run-down time t (b) of the braking torque M during the free run-down of the turbocharger (crankshaft) rotor on the run-down time t.

In the run-down mode of the crankshaft with a closed throttle valve, an additional braking torque is created (line 2, Fig. 4) counteracting the rotation of the turbocharger (crankshaft) rotor, which can be presented in the form of the following equation:

$$J \cdot \left(\frac{d\omega}{dt} + \frac{d\omega_i}{dt} \right) = -M_M - M_A \quad (7)$$

where $\frac{d\omega_i}{dt}$ is the increment in the deceleration value caused by the slowdown of the air flow by the throttle valve (rad/s²); M_A is the additional moment of counteraction to the rotation of the turbocharger rotor (crankshaft) (N·m).

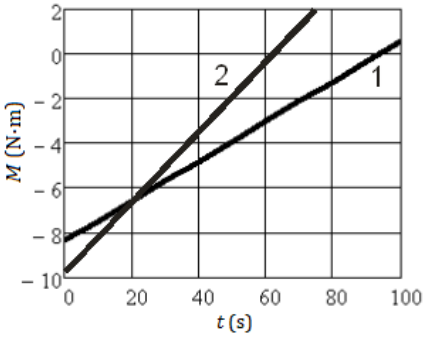

Fig. 4. The dependence of the braking torque M during the run-down of the turbocharger rotor (crankshaft) on the run-down time t: 1 – during a free run-down; 2 – during the run-down with a closed throttle valve.

The moment of resistance of the rotating ICE parts M_T is constant and almost does not depend on the angular speed [27]. With this in mind, the angular acceleration (deceleration) ε of the crankshaft is:

$$\varepsilon = \frac{d\omega}{dt} = -\frac{1}{j}(M_T + k\omega) \quad (8)$$

where ω is the angular rotation speed (rad/s); τ is the time interval (s); j is the moment of inertia of the rotating ICE parts: k is the degree of influence of ω on the friction coefficient.

The solution of differential equation (8) under the initial conditions $\omega=\omega_0$ and $\tau=0$ gives a dependence of ω on τ :

$$\omega = \frac{\varepsilon_0}{k} e^{-\frac{k}{j}\tau} - \frac{M_T}{k} \quad (9)$$

where ε_0 is the acceleration (deceleration) at the initial moment of time (τ=0):

The acceleration (deceleration) at the initial moment of time (τ=0) is:

$$\varepsilon_0 = -\frac{1}{j}\left(M_T + k\omega_0\right) \tag{10}$$

The run-down time (duration) τ_t is determined from expression (9), given that ω=0. After taking the logarithm and making transformations, we will obtain:

$$\tau_t = \frac{j}{k}\ln\left(\frac{-\varepsilon_0 j}{M_T}\right) \tag{11}$$

When measuring the run-down, the angular speed of the crankshaft can be written as follows:

$$\omega = \omega_0 e^{-a\tau} - \omega_d \tag{12}$$

where a is the design parameter; ω_d is the decrease in the angular speed of the rotor shaft due to the setting the additional exhaust resistance (rad/s).

The run-down time τ_t can be determined from expression (12) at ω=0 :

$$\tau_d = \frac{1}{a}\ln\frac{\omega_d}{\omega_0} \tag{13}$$

3. EXPERIMENTAL RESEARCH PROCEDURE

The experimental research procedure involved the development of a research motor complex, the preparation of a device to simulate the resistance in the exhaust system, and the use of a DBD-4 gasoline engine re-loader and USB Autoscope 4 (Postolovsky's oscilloscope) as diagnostic tools [29].

A motor unit based on the ZMZ-406.10 engine was used as a research motor complex. The ZMZ-406.2 engine is injection gasoline with fuel injection in front of the intake valve, 4-cylinder, 16-valve, with the cylinder diameter of 92 m and the piston stroke of 86 mm, with 1-3-4-2 cylinder operating order, subject to Euro-4 environmental standards (Fig. 5a).The device to simulate the resistance in the exhaust system (Fig. 5b) is a nozzle with replaceable disks of calibrated sections.

The diagnostic tools - DBD-4 gasoline engine re-loader and USB Autoscope 4 (Postolovsky's oscilloscope) are shown in Figs. 6a and 6b, respectively.

(a)

(b)

Fig. 5. Test object (a) research motor complex (b) devices to simulate the resistance in the exhaust system.

(a)

(b)

Fig. 6. Diagnostic tools (a) DBD-4 gasoline engine re-loader (b) USB Autoscope 4 (Postolovsky's oscilloscope).

During the experimental studies, we used the diagnostic equipment based on the DBD-4 gasoline engine re-loader. DBD-4 implements the function of test loading due to complete and partial shutdown of sparking and fuel supply. DBD-4 is connected to the gap of the power socket of electromagnetic injectors and ignition system modules. The operating principle of this tool is to simulate a static load by loading with the power of the mechanical losses of the disconnected cylinders. The control interface of the diagnostic program of the DBD-4 diesel engine re-loader is shown in Fig. 7.

Figure 7 shows the control interface, which has the fuel supply/sparking off buttons, partial fuel supply/sparking off buttons, buttons to control the composition of the fuel-air mixture and the ignition timing, as well test mode control buttons. Besides, important output parameters are displayed in the lower part of the interface: revolutions - the current value of the ICE crankshaft speed is 3320 rpm; temperature – the current operating temperature of the coolant is 93 °C; throttle - the current throttle opening percentage is 98 %; IDA correction – the correction of the ignition dwell angle (if the value of the IDA is added to the standard value) is 10 degrees; current position of the AAV – the position of the auxiliary air valve is 99 steps; fuel consumption – the instant fuel consumption is 23.2 l/h. All the parameters change with high resolution in the current time interval.

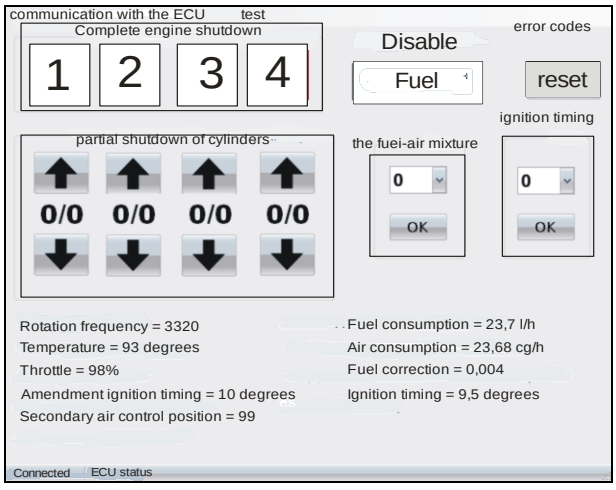

Fig. 7. The control interface of the diagnostic program of the DBD-4 diesel engine re-loader.

USB Autoscope 4 (Postolovsky's oscilloscope) was used to control the parameters of the run-down time and the number of revolutions made by the crank-shaft until the ICE stopped completely. During the implementation of the experimental research, we set the value of the specified ICE speed at the level of 5,500 rpm, or any other value. Simultaneously with the current ICE operation process, we ensured the start of the USB Autoscope 4 oscillogram sweep, Fig. 8.

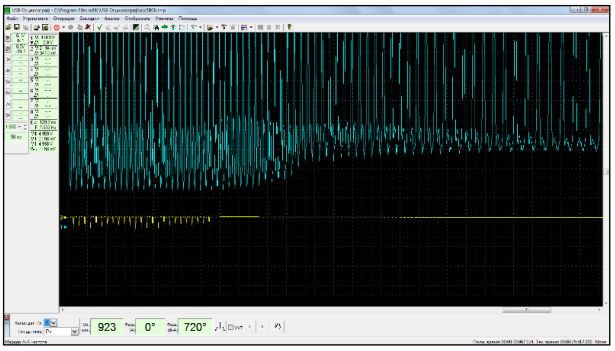

Fig. 8. A recorded current sweep of the USB Autoscope 4 oscillogram: 1 – change in the instantaneous pressure value in the first cylinder of the ICE; 2 – change in the signal of the primary circuit of the ignition system.

The USB Autoscope 4 oscillogram sweep was started simultaneously with the ICE. Then, the initial value of the ICE crankshaft speed was set, the recording was turned on, after which the ignition was simultaneously turned off and the ICE crankshaft was run down to a complete stop in the recording mode. After the ICE stopped completely, the recording was stopped and the current time section was saved in the memory of a computer device connected to USB Auto-scope 4.

The experimental data was processed for three run-down variants: 1) with a free run-down of the ICE crankshaft and a fully closed throttle valve; 2) with a free run-down of the ICE crankshaft and a 100 % open throttle valve; 3) with a free run-down of the ICE crankshaft and the installation of various measuring orifices (formation of artificial resistance) in the exhaust system and a 100 % open throttle valve.

4. EXPERIMENTAL RESEARCH RESULTS

Let us consider an experimental dependence of the run-down time t on the equivalent diameter of the exhaust pipe d, mm, provided that the run-down begins: 1) from 5,000 rpm; 2) from 4,000 rpm; 3) from 3,000 rpm (Fig. 9).

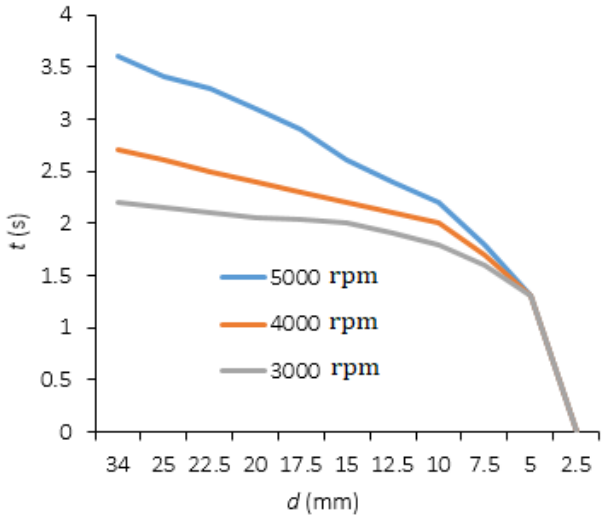

Fig. 9. The dependence of the run-down time t on the equivalent diameter of the exhaust pipe d provided that the run-down begins: 1) from 5,000 rpm; 2) from 4,000 rpm; 3) from 3,000 rpm.

Let us consider the conditions for implementing the dependence in Fig. 9. Before making measurements on a running engine, the gas pedal sets the initial value of the ICE crankshaft speed. During the test, when the specified initial ICE crankshaft speed is reached, the gas pedal is fixed, and the stability of the ICE crankshaft speed readings is achieved. After reaching the specified (stable) value of the ICE crankshaft speed, the screen shows the red speed value, Fig. 7. After that, the gas pedal is completely released, and the engine runs down to a complete stop (the throttle valve is a factor of slowing down the air flow) (Fig. 9).

As we can see from Fig. 9, the maximum difference in the values of the run-down time is observed at an equivalent diameter of the exhaust pipe d=34 mm (which corresponds to the nominal value of the exhaust gas tract resistance). However, the slope angle of the run-down time dependences is slightly different. So, for high initial ICE crankshaft speeds, the slope angle is larger. In the range from d=34 mm to 10 mm, the run-down time actually varies linearly. After passing the point corresponding to d=10 mm, the slope angle of the dependences sharply increases and coincides for all the three run-down variants mentioned above. However, al-ready at the point d=10 mm, a critical variant of the exhaust gas tract resistance is recorded, after which it is impossible to set the initial ICE crankshaft speed at the level of 5,000, 4,000, and 3,000 rpm. The balance point is observed at a lower speed. As shown by numerous experiments, the zone of equivalent cross-sections less than 10 mm is critical, after which the ICE operation is complicated or completely impossible.

It is worthy to consider the dependence of the run-down time t on the initial ICE crankshaft speed k at different values of the equivalent diameter of the exhaust pipe d Fig. 10.

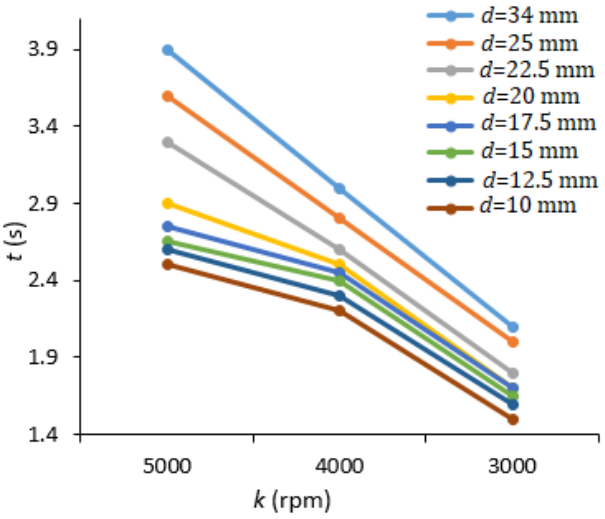

Fig. 10. The dependence of the run-down time t on the initial ICE crankshaft speed k at different values of the equivalent diameter of the exhaust pipe d.

As we can see from Fig. 10, with an increase in the exhaust gas duct resistance (with a decrease in the equivalent cross-section), the ICE run-down time decreases, wherein the dynamics of the decrease in the run-down time is most significant at the beginning of the resistance growth process.

So, the difference in the run-down time between two neighbouring dependences is Δt=0.3 s at a decrease in the equivalent cross-section from 34 to 25 mm. At a decrease in the equivalent diameter of the exhaust pipe below d=20 mm, the decrease in the run-down time becomes less noticeable. The difference of the run-down time between two neighbouring dependencies becomes less Δt=0.1 s.

An important diagnostic parameter is the total number of revolutions N before the engine stops. Fig. 11 shows the dependence of the total number of revolutions N before the engine stops on the equivalent diameter of the exhaust pipe d provided that the run-down begins from 5,000 rpm.

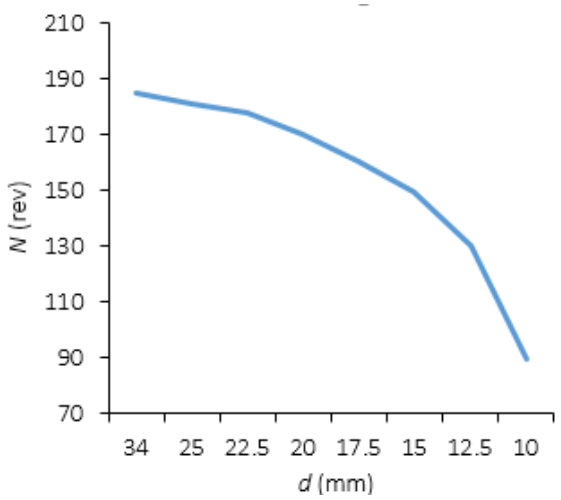

Fig. 11. The dependence of the total number of revolutions *N* before the engine stops on the equivalent diameter of the exhaust pipe *d* provided that the run-down begins from 5,000 rpm.

We can see from Fig. 11 that in the initial variation range of the equivalent diameter of the exhaust pipe *d*=34-15 mm, the dependence is almost linear. However, below the value *d*=15 mm, the dependence dynamically bends downward, and at 10 mm the condition for the beginning of the run-down from 5,000 rpm is not observed. That is, the engine is no longer gaining such high revolutions. The more the resistance of the exhaust gas tract, the lower falls the stable possible crankshaft speed at the beginning of the run-down.

As we can see from Fig. 12, the dependence of the run-down time *t* on the equivalent diameter of the exhaust pipe *d* provided that the run-down begins from 5,000 rpm, has a downward tendency, dynamically decreasing closer to 10 mm.

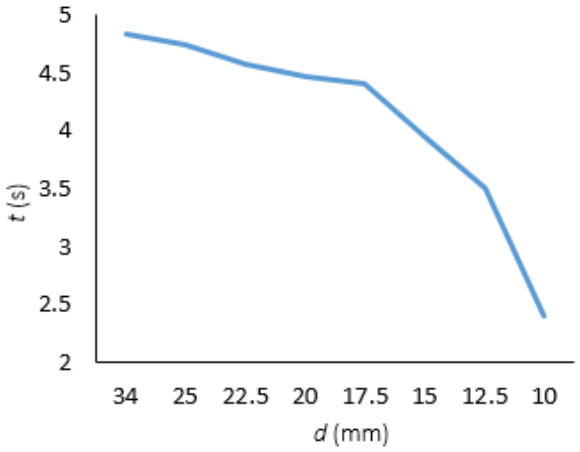

Fig. 12. The dependence of the run-down time *t* on the equivalent diameter of the exhaust pipe *d* provided that the run-down begins from 5,000 rpm.

A peculiar feature of the dependence in Fig. 12 is the run-down control condition: at the zero point of the run-down, the throttle valve is kept fully open throughout the run-down, until the ICE crankshaft stops completely. In Fig. 12, the gas pedal is held during the test until setting the desired speed. At the zero point of the run-down, it is kept fully pressed throughout the run-down, until the ICE crankshaft stops completely. This creates a minimum resistance to the air movement and the run-down time is slightly increased as compared to the variant of the run-down control with the throttle valve closed. The dependence in Fig. 12 is very demonstrative and can be used in the practice of determining the technical condition of the exhaust system at any stage of the car and motor machinery operation.

4.1 Determining the technical condition of the exhaust system

We carried out experimental studies to assess the degree of changes in the concentration of exhaust gas components. The input parameters were the capacity of the electromagnetic injector and the equivalent section of the catalytic converter. The capacity of the electromagnetic injector was estimated in % of the nominal capacity (for a new electromagnetic injector). The 100 % value was taken for a new injector. We also used electromagnetic injectors with a 6 % increase in a 6 % decrease in the capacity. The equivalent section of the catalytic converter was estimated in mm of the diameter. The range was chosen taking into account the nominal resistance of the catalytic converter and its limiting value of 34-10 mm. During the experimental studies, the engine was brought to the following operating mode: one cylinder on, the other three cylinders off; 20 % opening of the throttle valve, the operating temperature of the coolant is 90 °C; the spark plug gap was set constant and equal to 1.1 mm. The estimated parameters were the engine speed, the oxygen concentration, the carbon dioxide concentration, the carbon monoxide concentration, and the hydrocarbon concentration.

According to the experiment data, we built a graphical dependence of the ICE crankshaft speed on the resistance of the catalytic converter and the capacity of the electromagnetic injector with a spark plug gap *Z*=1.1 mm (Fig. 13).

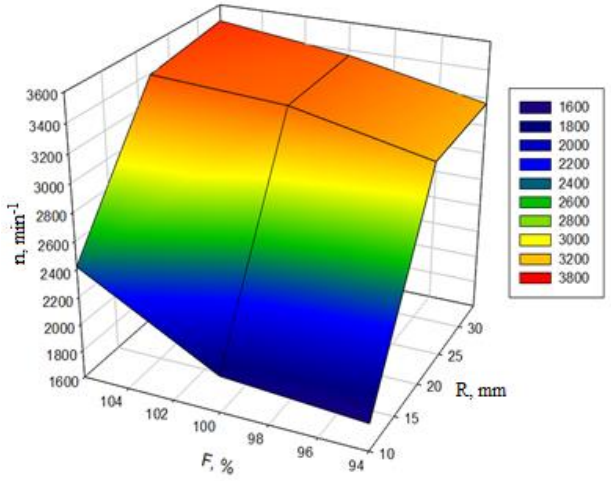

Fig. 13. The dependence of the ICE crankshaft speed on the resistance of the catalytic converter and the capacity of the electromagnetic injector at a constant value of the spark plug gap *Z*=1.1 mm.

The dependence in Fig. 13 is approximated by the following quadratic equation:

$$n(R,F) = 8259.3 + 237.12 \cdot R - 197.87 \cdot F - \\ - 4.15 \cdot R^2 + 1.15 \cdot F^2 \quad (14)$$

We can see from the obtained graphical dependence (Fig. 13) that at the minimum resistance of the catalytic converter of 10 mm and the nominal capacity of the electromagnetic injector of 100 %, the ICE crankshaft speed is minimal. This is preconditioned by the accumulation of exhaust gases in the exhaust system and the growing backpressure; at such combination of factors, the ICE crankshaft speed amounted to 1,870 rpm. This dependence indicates a malfunction of the exhaust system elements (increased resistance of the catalytic converter).

The minimum ICE crankshaft speed is observed at a minimum resistance of the converter of 10 mm and a capacity of the electromagnetic injector of 94 %. Such a response of the ICE is connected with weak running and an increase in the backpressure in the exhaust system. The maximum ICE crankshaft speed is observed at a nominal exhaust system resistance of 34 mm and a maximum capacity of the electromagnetic injector of 106 %, the engine crankshaft speed with this combination of factors was 3,480 rpm. The ICE response towards the maximum crankshaft speed indicates that the fuel-air mixture is superrich. In the graph inflection area, the equivalent section of the catalytic converter is 22 mm, and the capacity of the electromagnetic injector is 94 %. The exhaust gas backpressure factor starts to influence in this area.

According to the data of the experimental studies, we built a graphical dependence of the O_2 concentration on the resistance of the catalytic converter and the capacity of the electromagnetic injector with a spark plug gap *Z*=1.1 mm (Fig. 14).

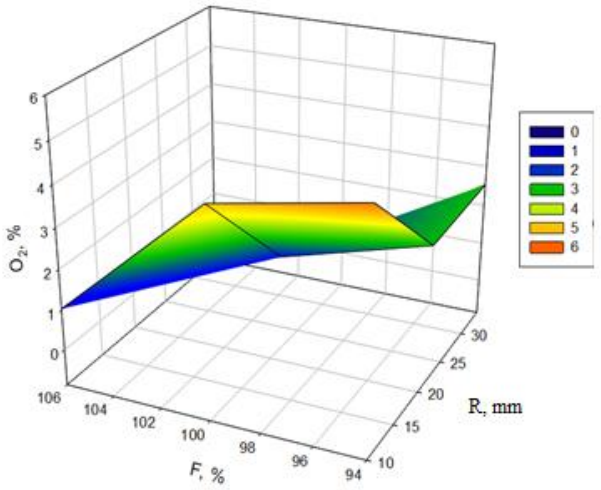

Fig. 14. The dependence of the O_2 concentration on the resistance of the catalytic converter and the capacity of the electromagnetic injector at a constant value of the spark plug gap Z=1.1 mm.

The dependence in Fig. 14 is approximated by the following equation:

$$O_2(R,F) = 4.74 - 0.33 \cdot R + 0.26 \cdot F + \\ + 0.005 \cdot R^2 - 0.002 \cdot F \quad (15)$$

It follows from the analysis of the presented graph in Fig. 14 that at the capacity of the injector of 94 % and the resistance of the catalytic converter of 10 mm, the oxygen content in the exhaust gas sample is maximum and equal to 4.92 %. This indicator is connected with complete combustion of the lean mixture and the accumulation of exhaust gases in the exhaust gas tract, which directly indicates a malfunction of the exhaust gas after-treatment system. At the resistance of the catalytic converter of 22 mm and the capacity of the injector of 94 %, the O_2 indicator noticeably drops to 2.48 % in the graph, which indicates low fuel content in the air-fuel mixture and an increased resistance of the exhaust gas tract. At a nominal resistance of the converter of 34 mm and a minimum capacity of the electromagnetic injector of 94 %, we observe an increase in the O_2 content to 2.53 %,

which directly indicates a malfunction of the fuel supply system.

At the nominal flow rate of the fuel injector of 100 % and the maximum resistance of the catalytic converter of 10 mm, we recorded an increased O_2 content in the exhaust gas sample equal to 4.24 %, which indicates a malfunction of the exhaust system. At the maximum capacity of the electromagnetic injector of 106 % and the resistance of the catalytic converter of 10 mm, we observed a sharp drop in the percentage content of O_2 to 1.04 %. Such a sharp drop indicates the richest air-fuel mixture and a malfunction of the electromagnetic injector. At the nominal capacity of the electromagnetic injector of 100 % and the nominal resistance of the converter of 34 mm, we recorded the O_2 value of 0.34 %, which indicates the optimal combustion of the air-fuel mixture.

According to the experimental studies, we built a graphical dependence of the CO_2 concentration on the resistance of the catalytic converter and the capacity of the electromagnetic injector with a spark plug gap Z=1.1 mm (Fig. 15).

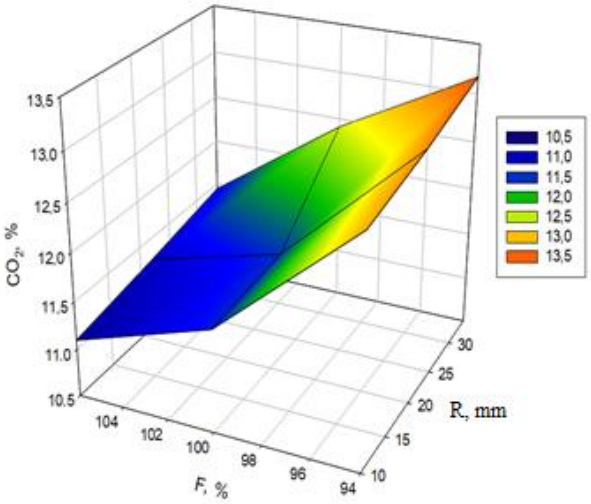

Fig. 15. The dependence of the CO_2 concentration on the resistance of the catalytic converter and the capacity of the electromagnetic injector at a constant value of the spark plug gap Z=1.1 mm.

The dependence in Fig. 15 is approximated by the following equation:

$$CO_2(R,F) = 98.8 - 0.01 \cdot R - 1.59 \cdot F + \\ + 0.0009 \cdot R^2 + 0.007 \cdot F^2 \quad (16)$$

We can see from Fig. 15 that the minimum CO_2 values are reached at the maximum capacity of the electromagnetic injector of 106 % and the maximum resistance of the catalytic converter of 10 mm. The CO_2 content in the exhaust gas sample with this ratio of factors was 11.1 %, which indicates incomplete combustion of the air-fuel mixture and a malfunction of the electromagnetic injector. There is a graph curvature in the area of the nominal capacity of the electromagnetic injector of 100 % and the resistance of the converter of 10 mm. In this area, the percentage content of CO_2 is 11.57 %, which indicates the optimal supply of the air-fuel mixture.

According to the results of the experiment, we built a graphical dependence of the CO concentration on the resistance of the catalytic converter and the capacity of the electromagnetic injector with a spark plug gap Z=1.1 mm (Fig. 16).

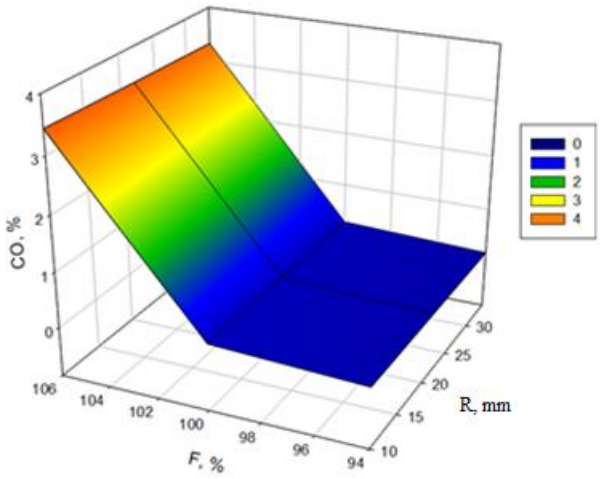

Fig. 16. The dependence of the CO concentration on the resistance of the catalytic converter and the capacity of the electromagnetic injector at a constant value of the spark plug gap Z=1.1 mm.

The dependence in Fig. 16 is approximated by the following equation:

$$CO\ (R,F) = 388.3 - 0.003 \cdot R - 8.02 \cdot F + \\ + (2.3E - 0.05) \cdot R^2 + 0.04 \cdot F^2 \quad (17)$$

An analysis of Fig. 16 shows that at the minimum supply of the electromagnetic injector of 94 % and the maximum resistance of the catalytic converter, there is complete combustion of the air-fuel mixture for these extreme conditions, while the CO content is at the level of 0.19 %. In the range of the capacity of the electromagnetic injector from 94 % to 100 % and the equivalent section of the catalytic converter from 10 to 34

mm, we observed a consistently low CO content. With an increase in the capacity of the electromagnetic injector to 106 %, there is a sharp increase in the CO content in the exhaust gas sample, which is connected with poor combustion of the air-fuel mixture due to its re-enrichment, which leads to the highest CO content of 3.44 %. The highest CO value indicates a malfunction of the electromagnetic injector.

According to experimental studies, we built a graphical dependence of the CH concentration, ppm on the resistance of the catalytic converter and the capacity of the electromagnetic injector with a spark plug gap Z = 1.1 mm (Fig. 17).

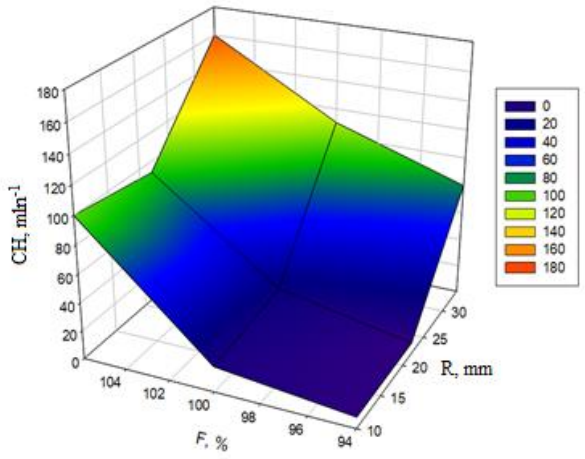

Fig. 17. The dependence of the CH concentration on the resistance of the catalytic converter and the capacity of the electromagnetic injector at a constant value of the spark plug gap Z = 1.1 mm.

The dependence in Fig. 17 is approximated by the following equation:

$$CH(R,F) = 5853.8 - 8.29 \cdot R - 122.5 \cdot F + \\ + 0.25 \cdot R^2 + 0.64 \cdot F^2 \quad (18)$$

We can see from the presented dependence in Fig. 17 that at the capacity of the electromagnetic injector of 94 % and the equivalent section of the catalytic converter of 10 mm, we observe the minimum CH content in the exhaust gas sample equal to 8 ppm, which indicates complete combustion of the air-fuel mixture. With an increase in the capacity of the electromagnetic injector and a decrease in the converter resistance, we observe an increase in the CH content in the exhaust gas sample, which indicates incomplete combustion of the air-fuel mixture. At the maximum capacity of the electromagnetic injector of 106 % and the nominal capacity of the catalytic converter, we observe the maximum CH content of 160 ppm in the exhaust gas sample, which indicates a malfunction of the fuel supply system (increased capacity of the electromagnetic injector).

The developed method can be used to determine the condition of a gasoline or diesel particulate filter without dismantling it from the car. The use of this method allows one to monitor the technical condition of the catalytic converter if it is damaged or missing, as well as with an empty filter, full and overfilled state of the filter to be regenerated.

5. CONCLUSION

The profound analysis of the tools and methods for diagnosing exhaust systems has shown that the effectiveness of the diagnostic technologies and tools is insufficient. We established that an alternative method for increasing the efficiency of the diagnostics process is the diagnostics based on the ICE run-down time value. To implement the proposed diagnostic method, we developed a research motor complex; a device to simulate the resistance in the exhaust system; DBD-4 loader for gasoline engines, and USB Autoscope 4 (Postolovsky's oscilloscope). When carrying out the experimental studies and processing the obtained data, we established that the run-down time can be taken as a sensitive diagnostic parameter to determine the technical condition of the exhaust system. The experimental data were processed for three run-down variants: 1) with a free run-down of the ICE crankshaft and a fully closed throttle valve; 2) with a free run-down of the ICE crankshaft and a 100 % open throttle valve; 3) with a free run-down of the ICE crankshaft and installation of various measuring orifices (formation of artificial resistance) in the exhaust system and a 100 % open throttle valve.

When analyzing the experimental dependence of the run-down time on the equivalent diameter of the outlet pipe provided that the run-down starts from 5,000 rpm, 4,000 rpm, and 3,000 rpm, the maximum difference in the run-down time values was established at the equivalent diameter of the exhaust pipe d=34 mm (which corresponds to the nominal value of the exhaust gas tract resistance). After passing the point corresponding to d=10

mm, the slope angle of the dependences sharply increases and coincides for all the aforesaid three run-down variants. However, already at the point *d*=10 mm, we observe a critical variant of the exhaust gas tract resistance, after which it is impossible to set the initial ICE crankshaft speed at the level of 5,000, 4,000, and 3,000. The balance point is observed at a lower speed. As shown by the numerous experiments, the area of equivalent sections less than 10 mm is critical, after which the ICE operation is complicated or completely impossible.

REFERENCES

[1] N.R. Martin, P. Kelley, R. Klaski, A. Bosco, B. Moore, N. Traviss, *Characterization and Comparison of Oxidative Potential of Real-World Biodiesel and Petroleum Diesel Particulate Matter Emitted from a Nonroad Heavy Duty Diesel Engine*, Science of the Total Environment, vol. 655, pp. 908-914, 2019, doi: 10.1016/j.scitotenv.2018.11.292

[2] Q. Li, A. Wyatt, R.M. Kamens, *Oxidant Generation and Toxicity Enhancement of Aged-Diesel Exhaust*, Atmospheric Environment, vol. 43, iss. 5, pp. 1037-1042, 2009, doi: 10.1016/j.atmosenv.2008.11.018

[3] L. De Oliveira Costa, R.S. Santos, *New Challenges and Technologies for the Emissions Monitoring System (OBD) in Heavy Duty Diesel Engines to Meet the Requirements of the PROCONVE P7*, SAE Technical Papers, 2012, doi: 10.4271/2012-36-0245

[4] A. Rimkus, S. Stravinskas, J. Matijošius, *Comparative Study on the Energetic and Ecologic Parameters of Dual Fuels (Diesel-NG and HVO-Biogas) And Conventional Diesel Fuel in a CI Engine,* Applied Sciences, vol. 10, iss. 1, p. 359, 2020, doi: 10.3390/app10010359

[5] C. Pana, N. Negurescu, M.G. Popa, Al. Cernat, *Ecologic Automotive Diesel Engine Achieved* by *LPG Fuelling,* Journal of Environmental Protection and Ecology, vol. 13, no. 2, pp. 688-699, 2012.

[6] C. Pană, N. Negurescu, M.G. Popa, G. Pop, R. Ganea, N. Natu, C. Teodorescu, *Dimethylether - Ecological Fuel for Diesel Engines [Dimetil eter - Combustibil ecologic pentru motoare Diesel*], Revista de Chimie, vol. 55, no. 4, pp. 253-258, 2004.

[7] G. Gonca, B. Sahin, *Thermo-Ecological Performance Analyses and Optimizations of Irreversible Gas Cycle Engines,* Applied Thermal Engineering, vol. 105, pp. 566-576, 2016, doi: 10.1016/j.applthermaleng.2016.03.046

[8] R. Gennish, J. Jiang, A. Albarbar, G. Harris, F. Gu, A. Ball, *Diesel engine combustion monitoring based on acoustic measurement of exhaust systems*, in 8th Biennial ASME Conference on Engineering Systems Design and Analysis, 4-7 July, 2006, ESDA 2006.

[9] J. Jiang, F. Gu, R. Gennish, D.J. Moore, G. Harris, A.D. Ball, *Monitoring of Diesel Engine Combustions Based on the Acoustic Source Characterisation of the Exhaust System,* Mechanical Systems and Signal Processing, vol. 22, iss. 6, pp. 1465-1480, 2008, doi: 10.1016/j.ymssp.2007.12.003

[10] G. Yao, H. Wu, Z. Guo, X. Zi, A *Research on the Remote Monitoring Technology of Exhaust After-Treatment System in Diesel Vehicle*, Qiche Gongcheng/Automotive Engineering, vol. 36, no. 7, pp. 824-827, 2014.

[11] R. De Matos, E. Foltête, N. Bouhaddi, B. Poutot, *Characterization of the dynamic behavior of car exhaust purification systems,* in the 23rd Conference and Exposition on Structural Dynamics, 31 January - 3 February, 2005, Orlando, Conference Proceedings of the Society for Experimental Mechanics Series, p. 8.

[12] T. Morita, N. Suzuki, N. Satoh, K. Wada, H. Ohno, *Study on low NOX emission control using newly developed lean NOX catalyst for diesel engines,* in the 2007 World Congress, 16-19 April, 2007, Detroit, SAE Technical Papers, doi: 10.4271/2007-01-0239

[13] D.A. Burgard, M.N. Provinsal, *On-road, In-Use Gaseous Emission Measurements by Remote Sensing of School Buses Equipped with Diesel Oxidation Catalysts and Diesel Particulate Filters,* Journal of the Air and Waste Management Association, vol. 59, iss. 12, pp. 1468-1473, 2009, doi: 10.3155/1047-3289.59.12.1468

[14] Z.G. Liu, J.C. Wall, P. Barge, M.E. Dettmann, N.A. Ottinger, *Investigation of PCDD/F Emissions from Mobile Source Diesel Engines: Impact of Copper Zeolite SCR Catalysts and Exhaust Aftertreatment Configurations*, Environmental Science and Technology, vol. 45, iss. 7, pp. 2965-2972, 2011 doi: 10.1021/es103933e

[15] Y. Liu, M. Qiao, S. Jia, *Anomaly detection for health assessment and prediction of diesel generator set,* in 4th International Conference on Communication and Information Processing, 2-4 November, 2018, ICCIP 2018, Ocean University of ChinaQingdao, ACM International Conference Proceeding Series, pp. 212-216.

[16] R. Zadrąg, T. Kniaziewicz, *Evaluation of the engine technical condition based on criterial analysis of exhaust emission indicators*, Transportation

Research Procedia, vol. 40, pp. 940-948, 2019, doi: 10.1016/j.trpro.2019.07.132

[17] Y.V. Chepurnyi, O.M. Leonenko, *The Method of Controlling the Valve Mechanism of the Engine for Exhaust Pulsation Experimental Study*, International Journal on Emerging Technologies, vol. 11, no. 3, pp. 91-95, 2020.

[18] B.J. Murphy, M.S. Lebold, K. Reichard, T. Galie, C. Byington, *Diagnostic fault detection for internal combustion engines via pressure curve reconstruction,* in IEEE Aerospace Conference, 8-15 March, 2003, Big Sky, IEEE Aerospace Conference Proceedings, vol. 7, no. 1234167, pp. 3239-3246, doi: 10.1109/AERO.2003.1234167

[19] B.M. Dawson, M.A. Franchek, K. Grigoriadis, R.W. McCabe, S.B. Smith, A *systematic method for automotive three-way catalyst diagnostics: Experimental results,* in 2008 ASME Dynamic Systems and Control Conference, 20-22 October, 2008, DSCC 2008, Ann Arbor, pp. 323-329.

[20] D. Antory, Application of a *Data-Driven Monitoring Technique to Diagnose Air Leaks in an Automotive Diesel Engine: A Case Study,* Mechanical Systems and Signal Processing, vol. 21, iss. 2, pp. 795-808, 2007, doi: 10.1016/j.ymssp.2005.11.005

[21] M. Desbazeille, R.B. Randall, F. Guillet, M. El Badaoui, C. Hoisnard, *Model-based Diagnosis of Large Diesel Engines Based on Angular Speed Variations of the Crankshaft*, Mechanical Systems and Signal Processing, vol. 24, iss. 5, pp. 1529-1541, 2010, doi: 10.1016/j.ymssp.2009.12.004

[22] F. Kimmich, A. Schwarte, R. Isermann, *Fault Detection for Modern Diesel Engines Using Signal- And Process Model-Based Methods,* Control Engineering Practice, vol. 13, iss. 2, pp. 189-203, 2005, doi: 10.1016/j.conengprac. 2004.03.002

[23] C.A. Montes, P. Pisu, *Fault Detection in Idle Speed Control of IC Engines*, SAE Technical Papers, 2009, doi: 10.4271/2009-01-0729

[24] R. Gennish, J. Jiang, A. Albarbar, G. Harris, F. Gu, A. Ball, *Diesel engine combustion monitoring based on acoustic measurement of exhaust systems,* in 8th Biennial ASME Conference on Engineering Systems Design and Analysis, 4-7 July, Torino, ESDA 2006, pp. 567-574, doi: 10.1115/esda2006-95648

[25] Z.P. You, W.H. Zhang, X.P. Ye, *Diesel engine inlet and exhaust system fault detection based on PSO-BP NN*, Applied Mechanics and Materials, vol. 599-601, pp. 918-921, 2014, doi: 10.4028/www.scientific.net/AMM.599-601.918

[26] K. Ekinci, Ş. Ertuğrul, *Model Based Diagnosis of Oxygen Sensors,* IFAC-PapersOnLine, vol. 52, iss. 5, pp. 185-190, 2019, doi: 10.1016/j.ifacol. 2019.09.030

[27] E.V. Ageev, A.Y. Altukhov, A.V. Scherbakov, A.N. Novikov, *Informativeness Increasing of Internal Combustion Engines Diagnosis Due to Technical Endoscope,* Journal of Engineering and Applied Sciences, vol. 12, iss. 4, pp. 1028-1030, 2017, doi: 10.3923/jeasci.2017.1028.1030

[28] D. Ya. Nosyrev, A. A. Svechnikov, Yu. Yu. Stanovova, *Experimental Studies of the Turbocharger Operation at The Start of Rotation and at The Stop,* Vestnik transporta Povolzhya, vol. 1, no. 43, pp. 15-19, 2014. (in Russian)

[29] USB Postolovsky Oscilloscope (USB Autoscope IV) - software management instructions, available at: www.autoscaners.ru/upload/iblock/fec/autoscope_4_soft_manual_rus.pdf, accessed 19.08.2020